Petroleum Science 20 (2023) 1044–1052

Contents lists available at ScienceDirect

Petroleum Science

journal homepage: www.keaipublishing.com/en/journals/petroleum-science

Original Paper

Flow characteristics and regime transition of aqueous foams in porous media over a wide range of quality, velocity, and surfactant concentration

Bin-Fei Li [a, b, *], Meng-Yuan Zhang [a, b], Zhao-Min Li [a, b], Anthony Kovscek [c, **], Yan Xin [a, b], Bo-Liang Li [a, b]

[a] Key Laboratory of Unconventional Oil & Gas Development (China University of Petroleum (East China)), Ministry of Education, Qingdao, 266580, Shandong, PR China
[b] School of Petroleum Engineering, China University of Petroleum (East China), Qingdao, 266580, Shandong, PR China
[c] Department of Energy Resources Engineering, Stanford University, Stanford, CA, 94305, USA

ARTICLE INFO

Article history:
Received 9 February 2022
Received in revised form
16 November 2022
Accepted 18 November 2022
Available online 20 November 2022

Edited by Yan-Hua Sun

Keywords:
Foam flow regime and transition
Porous media
Pressure gradient
Flow velocity
Surfactant concentration
Foam quality

ABSTRACT

Aqueous foam is broadly applicable to enhanced oil recovery (EOR). The rheology of foam as a function of foam quality, gas and liquid velocities, and surfactant concentration constitute the foundation of its application. The great variations of the above factors can affect the effectiveness of N_2 foam in EOR continuously in complex formations, which is rarely involved in previous relevant studies. This paper presents an experimental study of foam flow in porous media by injecting pre-generated N_2 foam into a sand pack under the conditions of considering a wide range of gas and liquid velocities and surfactant concentrations. The results show that in a wide range of gas and liquid velocities, the pressure gradient contours are L-shaped near the coordinate axes, but V-shaped in other regions. And the surfactant concentration is a strong factor influencing the trend of pressure gradient contours. Foam flow resistance is very sensitive to the surfactant concentration in both the high- and low-foam quality regime, especially when the surfactant concentration is less than CMC. The foam quality is an important variable to the flow resistance obtained. There exists a transition point from low- to high-quality regime in a particular flow system, where has the maximum flow resistance, the corresponding foam quality is called transition foam quality, which increases as the surfactant concentration increases. The results can add to our knowledge base of foam rheology in porous media, and can provide a strong basis for the field application of foams.

1. Introduction

Foam is a dispersion of nonwetting phase, such as gas, within a continuous liquid phase where the dispersion is stabilized by surfactant (Li et al., 2017; Sarhan et al., 2018b; Johnson et al., 2022). As a type of compressible non-Newtonian fluid (Sarhan et al., 2018c), foam has very broad application prospects in porous media including the development of oil and gas fields because of unique foam structural and rheological characteristics (Wang et al., 2022). Foam has been referred to as an intelligent oilfield fluid.

Foam is widely applied in mineral flotation (Sarhan et al., 2016, 2017a, 2018a) or enhanced oil recovery (EOR) (Li et al., 2019; Ding et al., 2021; Sun et al., 2021). In EOR, foam reduces gas mobility thereby improving areal and vertical sweep efficiency (Fernø et al., 2016; Singh and Mohanty, 2017; Lozano et al., 2021). Foam application can effectively alleviate viscous fingering and gravitational coverage issues attributed to the low density and viscosity of gas (Fernø et al., 2015; Gauteplass et al., 2015; Lv et al., 2017; Wang et al., 2019). In addition, foam can increase the flow resistance in high-permeability zones and promote the transfer of fluid to low-permeability areas (Roncoroni et al., 2021).

The flow characteristics of foam constitute the basis of its application (Sarhan et al., 2017b, 2018c; Chen et al., 2019). A suitable understanding of foam flow behavior is necessary to optimize its application (Sarhan et al., 2018d). Foam flow in porous media involves a complex two-phase flow process. Foam morphology has a great influence on the fluidity of foam (Sarhan et al., 2017c; Hematpur et al., 2018). The dynamic characteristics of lamellar coalescence and formation in porous media lead to the change of foam morphology

* Corresponding author. Key Laboratory of Unconventional Oil & Gas Development (China University of Petroleum (East China)), Ministry of Education, Qingdao, 266580, Shandong, PR China.
** Corresponding author.
E-mail addresses: libinfei999@126.com (B.-F. Li), kovscek@stanford.edu (A. Kovscek).

https://doi.org/10.1016/j.petsci.2022.11.014

during the flow process. Thus, all parameters that influence lamellar coalescence and formation in porous media (such as characteristics of porous media, type and concentration of surfactants, flow velocity, and foam quality) affect foam flow (Skauge et al., 2020). Many studies have been performed under different conditions.

In 1988, Khatib et al. found that the stability of foam bubbles in porous media depends on the capillary pressure (Khatib et al., 1988). Later, Farajzadeh et al. reported that there was a threshold for capillary pressure in foam generation, beyond which the foam could not survive, and they referred this capillary pressure as "limiting capillary pressure (P_c^*)" (Farajzadeh et al., 2015). Above this limiting capillary pressure, foam coalesces rapidly. P_c^* varies with parameters such as surfactant type and concentration (Kahrobaei and Farajzadeh, 2019). With the increase in the concentration of surfactant, the P_c^* increases, the foam stability increases, the flow resistance in the core increases, and a longer time is taken by the foam flow to reach stability (Wang and Li, 2016; Li et al., 2019).

Based on foam quality, foam inside the porous media is categorized into two strong foam and weak foam. Weak foam with coarse texture shows a moderate increase in differential pressure. However, strong foam with fine texture shows a large increase in differential pressure and decreases the gas mobility. Most of the results (Osterloh and Jante, 1992; Cheng et al., 2000; Alvarez et al., 2001; Kam et al., 2007; Buchgraber et al., 2012; Almajid and Kovscek, 2022) showed two distinct flow regimes in porous media: strong foam regime and weak foam regime. The pressure gradient is independent of the velocity of the liquid phase in the weak foam regime (low-quality regime), on the contrary, the pressure gradient is independent of the velocity of the gas phase in the strong foam regime (high-quality regime). Hence, an L-shaped contour for pressure gradient is obtained on a plot of gas versus liquid velocity.

Different flow states of foam in porous media are dominated by different mechanisms. Rossen and Wang (1997) proposed a model describing foam flow in the low-quality regime. This model assumes that the foam mobility is controlled not by foam coalescence and capillary pressure, but by trapping and mobilization of foam bubbles of a fixed size. The bubble size is independent of the liquid and gas flow rates. Low-quality foam flow occurs under a certain yield stress, such as Bingham plastic foam flow under a fixed yield stress and plastic viscosity. Bubbles in a given porous medium do not flow unless the pressure gradient exceeds a certain threshold value that depends on the pore size or pore-throat diameter. Based on this model, the pressure drop should be a function of the pore geometry and surface tension. Alvarez et al. (2001) combined the limiting capillary pressure model and the above-mentioned model of Rossen and Wang to explain foam flow behavior in porous media. It was assumed that foam behavior is dominated by a single mechanism in each regime, namely, in the high-foam quality regime, foam behavior is determined by capillary pressure and coalescence, while in the low-foam quality regime, foam behavior is controlled by bubble trapping and mobilization. Based on this model, the pressure gradient contours exhibit a standard L shape, as shown in Fig. 1. Similar results have been reported in other studies of foam flow (Adebayo and Kanj, 2018; Simjoo and Zitha, 2020; Omirbekov et al., 2020; Yu et al., 2020).

According to this model, at a fixed gas flow rate, the pressure gradient increases with increasing liquid flow rate in region A, after which a transition point is reached. Then, the flow behavior transforms into the low-quality regime (region B), and the pressure gradient is independent of the liquid flow rate. In contrast, at a fixed liquid flow rate, the pressure gradient increases with increasing gas flow rate in region B, after which a transition point is reached. Subsequently, the flow process enters the high-quality regime (region A), and the pressure gradient becomes independent of the gas flow rate. The pressure gradient reaches its maximum value at

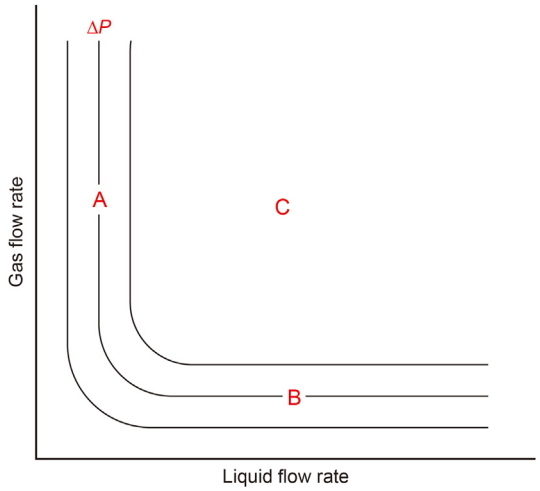

Fig. 1. Contours of the steady-state foam pressure gradient as a function of the gas and liquid flow rates. Region A is the so-called high-foam quality regime, and region B is the so-called low-foam quality regime.

the boundary between the high- and low-quality regions, and the foam quality at the transition point corresponding to the maximum pressure gradient is called transition foam quality (f_g^*), which varies with the type and concentration of surfactant and total flow rate (Kahrobaei et al., 2017; Tang et al., 2019; Rudyk et al., 2020). Kahrobaei and Farajzadeh (2019) investigated the effect of surfactant concentration on the transient and steady-state foam behavior in porous media. They found that as the surfactant concentration increases, the transition from the low-to high-quality regimes occurred at a larger foam quality. They also showed that the surfactant concentration affected only the high-quality regime, foam became stronger (or foam texture becomes finer) as the surfactant concentration increased (Kahrobaei and Farajzadeh, 2019).

As N_2 foam flows through complex formations, the variations over a wide range of flow velocity and surfactant concentration continue to affect its effectiveness in EOR. Therefore, it is of great significance to investigate the flow characteristics and regime transition of N_2 foam flow in porous media over a wide range of flow velocity and surfactant concentration. However, most of the previous studies focused on regions A and/or B, as shown in Fig. 1, indicating a low gas flow rate or low liquid flow rate near the coordinate axis, but not related to high-velocity regions. Moreover, previous studies of the effect of surfactant only involved the low-velocity region and were limited to the vicinity of CMC, especially there were few reports about the effect of surfactant on the regime transition of foam in porous media. The effect of surfactant on foam flow in porous media was obscure.

In this paper, we investigated foam flow characteristics and regime transition by injecting pre-generated N_2 foam into a sand pack under the conditions of considering a wide range of gas and liquid velocities and surfactant concentrations via laboratory experiments. We obtained pressure gradient contours in region C and the transition zone, and analyzed the transition between foam flow regimes over a wide range of velocities and the effects on the transition of surfactant concentration. The results of this study add to our knowledge base of foam rheology in porous media, and can provide a strong basis for the field application of foam fluid.

2. Experimental

2.1. Apparatus

Foam flow experiments were performed at different volumetric flow rates of gas and surfactant solution and increasing surfactant concentrations. Fig. 2 illustrates the experimental setup.

The experimental setup was designed in three parts to study foam flow behavior. The first part encompassed foam quality control and foam generation. Foam was pre-generated via co-injection of surfactant solution and N_2 into a sand pack, 12 cm in length and 0.4 cm in diameter. A constant-rate pump was employed to control the surfactant solution flow rate, and the gas flow rate was controlled by two gas mass flow controllers to obtain a wide range of gas flow rates. The second part aimed to measure the foam rheology in porous media. Another sand pack, which was 5 cm in length and 2.5 cm in diameter, was applied as the measurement porous medium (the mesh size of the sand was 120–160 mesh). Its permeability was 1.339 D and porosity was 32.6%. Foam exiting the foam generator flowed into the sand pack where pressure drop data was collected with pressure transducers. The third part was the foam flow visualization cell. At the downstream end of the sand pack, a visualization cell was connected to observe the foam characteristics. A digital microscope was adopted to capture images. At the outlet of the visualization cell, the effluent foam was discharged into a beaker and weighed to determine the flow rate of the surfactant solution.

The visualization cell comprised two transparent pieces of Plexiglas bolted together. A flow channel with a depth of 25 μm was created between the two pieces to provide a flow path for the generated foam. The channel was thin enough for the bubbles to flow in a single layer. A digital microscope captured the foam texture characteristics under different flow conditions. The foam texture was determined via postprocessing image analysis.

To obtain a wide range of gas flow rates, two gas mass flow controllers were applied. One device is an EL-FLOW Select Series mass flow meter/controller purchased from Bronkhorst, which is a thermal mass flow meter with a modular construction controlled by a computer. This mass flow controller is designed and calibrated for ultralow N_2 flow rates in the range from 0.001 to 0.7 mL/min. The other device is a Brooks mass flow controller 5850 Series, with a maximum flow rate of 10 mL/min.

2.2. Experimental materials

The surfactant used in the experiments was a sodium olefin sulfonate ($C_{14\text{-}16}$, from Stepan Company). The solution was prepared by adding different weight percentages of the surfactant to distilled water. The surface tension was measured to define the critical micelle concentration (CMC). Fig. 3 shows the surface tension as a function of the surfactant concentration. The inflection point at approximately 0.1 wt% indicates the CMC. The gas phase was N_2 in all experiments.

2.3. Experimental procedure

A series of experiments proceeded with the selection of the liquid and gas flow rates and surfactant concentrations. The liquid Darcy velocity in the sand pack ranged from 1 to 20.9 m/day. Accordingly, 6 gas velocity levels were selected for each liquid velocity to obtain different foam qualities and flow characteristics. The gas Darcy velocity reported here was computed at the average sand pack pressure because the pressure along the sand pack varied. The surfactant concentration ranged from 0.01 to 0.7 wt%.

The experiments were carried out under ambient temperature and pressure, and each experiment was conducted under conditions of constant liquid and gas injection rates and a constant outlet pressure. Steady-state flow was achieved in the sand pack under a constant pressure after the injection of 10 pore volumes (PV) of liquid. The steady state was chosen for data collection to analyze the effects of foam quality changes and saturation rebalancing. Once the measurements and observations in the steady state were completed, the next flow rate was selected to repeat the process.

3. Experimental results

Both surfactant concentration and gas and liquid flow rate can affect foam flow in porous media. The foam flow characteristics in porous media can be characterized by the pressure drop measured across the porous media. An overview of sand pack displacement with pre-generated N_2 foam experiments over a wide range of surfactant concentration, gas/liquid velocity, and foam quality was given in this section. And the effects of the above factors on foam flow in porous media were investigated by analyzing the changes of pressure gradient.

3.1. Pressure gradient

The pressure gradient was calculated based on the pressure drop along the sand pack and its length. A series of experiments were performed at different flow rates and surfactant concentrations. First, the surfactant concentration and liquid flow rate were

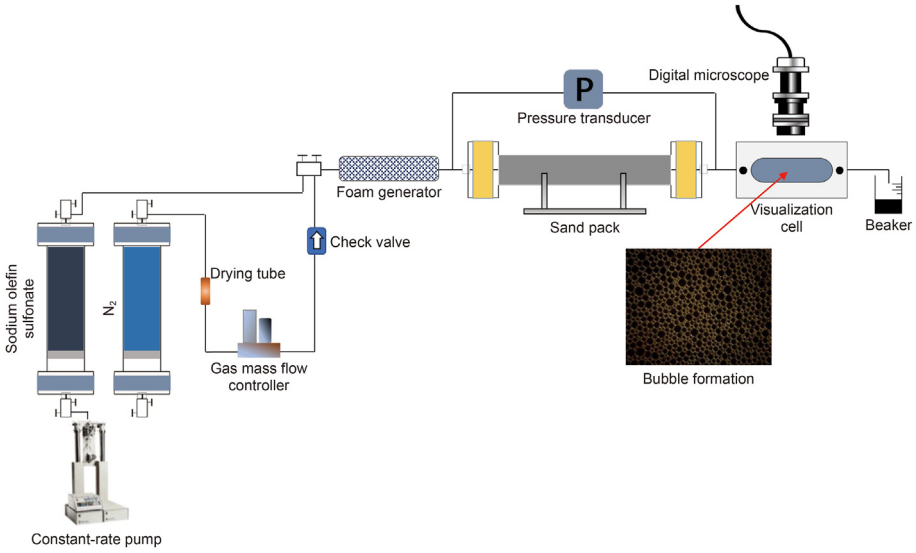

Fig. 2. Schematic of experimental apparatus.

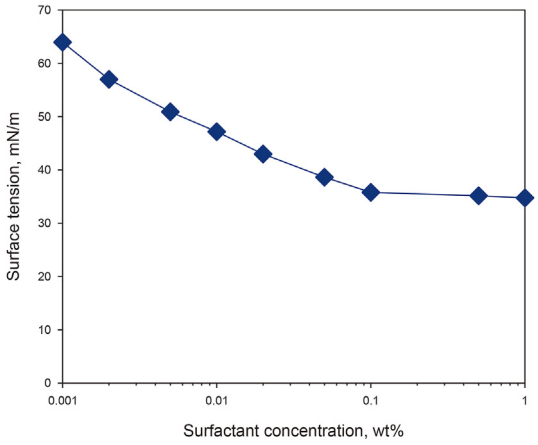

Fig. 3. Surface tension (mN/m) as a function of the surfactant concentration (wt%) in distilled water. The critical micelle concentration (CMC) is obtained at the inflection point.

fixed, and the gas flow rate was adjusted from low to high. The pressure drop between the inlet and outlet of the sand pack was measured in the steady state. Then, the liquid flow rate was changed, and accordingly, the gas flow rate was again adjusted from low to high. The foam quality ranged from 0.023 to 0.97. After the measurements were completed, a larger surfactant concentration was selected to repeat the process.

The pressure gradient contours like Fig. 4 obtained as a function of the liquid and gas Darcy velocities under steady-state conditions at the different surfactant concentrations, plotted via kriging interpolation. Pressure gradient data of the various liquid and gas flow rates were added on the coordinate axes. The upper-left region is the high-foam quality regime, and the lower-right region is the low-foam quality regime.

Fig. 4 shows pressure gradient contours as a function of the liquid and gas Darcy velocities under steady-state conditions at a surfactant concentration of 0.01 wt%. The figure shows that the pressure gradients are all less than 6.5×10^5 Pa/m within the measurement range. This indicates that foam can be generated in the porous medium at low surfactant concentrations, but the generated foam easily collapses at low surfactant concentrations due to the small limiting capillary resulting in a small maximum pressure gradient. In addition, the pressure gradient contours in Fig. 4 are L-shaped. At a high-foam quality, the pressure gradient declines with increasing gas velocity (the pressure contour lines move toward the right at high-foam quality). This phenomenon was first reported by Osterloh and Jante (1992). It was referred to as the chaotic regime.

Fig. 5 shows pressure gradient contour as a function of the liquid and gas Darcy velocities under steady-state conditions at a surfactant concentration of 0.1 wt%. The pressure gradient reaches 110×10^5 Pa/m within the measurement range. This is larger than the maximum pressure gradient at a surfactant concentration of 0.01 wt%. The surfactant concentration is now large enough to provide significant stability to foam lamellae. The limiting capillary pressure for foam coalescence is approaching or greater than the capillary pressure in the sand pack. Hence, the foam generated in the porous media remains relatively stable. In addition, Fig. 5 shows that the pressure gradient is almost insensitive to the gas velocity increase in the low-liquid velocity range and almost insensitive to the liquid velocity increase in the low-gas velocity range. The variation trend of the pressure gradient in the low-liquid velocity region or low-gas velocity region near the coordinate axis is basically consistent with that in Fig. 1, and the pressure gradient contours are all L-shaped. However, with increasing liquid and gas velocities, the pressure gradient contours tend to increase toward the upper-right region.

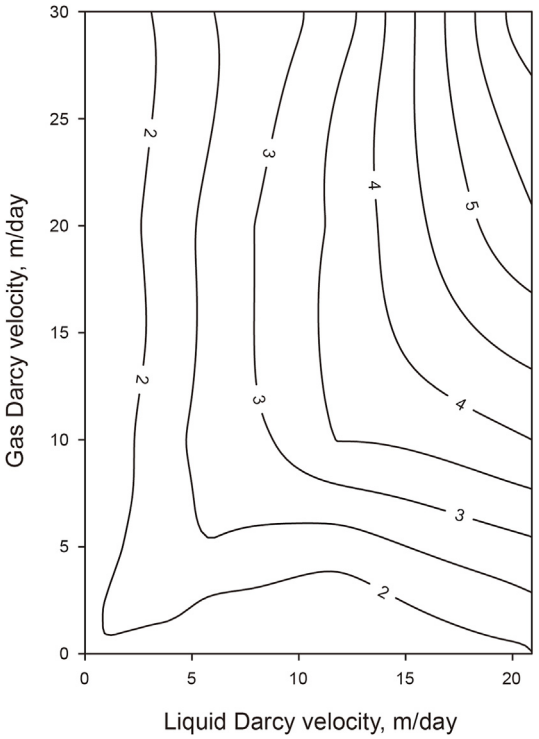

Fig. 4. Pressure gradient contours (10^5 Pa/m) as a function of the liquid Darcy velocity (m/day) and gas Darcy velocity (m/day) under steady-state conditions in porous media. The surfactant concentration is 0.01 wt%.

The pressure gradient respectively reaches 180×10^5 and 190×10^5 Pa/m within the measurement range at surfactant concentrations of 0.5 and 0.7 wt%. As anticipated, these values are all greater than that at a surfactant concentration of 0.1 wt%. In addition, the pressure gradient contours are similar at surfactant concentrations of 0.5 and 0.7 wt%, but the shapes of them are greatly different from those of the pressure gradient contours in Figs. 4 and 5. The variation trend of the pressure gradient in the low-liquid velocity region or low-gas velocity region near the coordinate axis is also substantially consistent with that in Fig. 1. Comparing Figs. 4 and 5, the pressure gradient contours near the coordinate axis are still L-shaped at surfactant concentrations of 0.5 and 0.7 wt %. However, with increasing liquid and gas velocities, they change to V-shaped curves in the other regions. In the small-liquid velocity range, the pressure gradient is almost insensitive to the gas velocity increase but is more sensitive to the liquid velocity than that at low surfactant concentrations of 0.01 and 0.1 wt%. Moreover, the effect of the gas velocity on the pressure gradient in the low-gas velocity range is obviously greater than that of the liquid velocity on the pressure gradient in the low-liquid velocity range at surfactant concentrations of 0.5 and 0.7 wt%, respectively.

Overall, the maximum pressure gradient within the measurement range increases with increasing surfactant concentration, especially as the concentration reaches the CMC. In addition, the variation trend of the pressure gradient in the region near the coordinate axis is similar under different surfactant concentrations, which is as follows: In the low-liquid velocity range, the pressure gradient is almost insensitive to the gas velocity increase but is sensitive to the liquid velocity. Similarly, in the low-gas velocity region, the pressure gradient is nearly insensitive to the liquid velocity increase but is sensitive to the gas velocity. L-shaped contours are observed in these regions. The results near the coordinate axis are in agreement with the previous studies but are different in the other regions at large surfactant concentrations which are greater

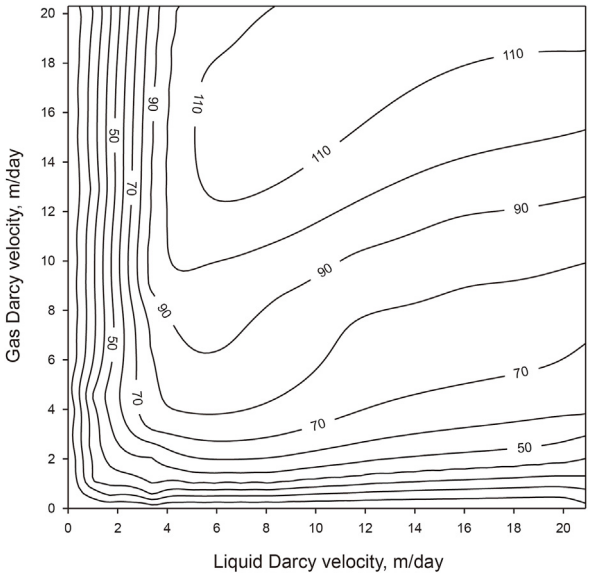

Fig. 5. Pressure gradient contours (10^5 Pa/m) as a function of the liquid Darcy velocity (m/day) and gas Darcy velocity (m/day) under steady-state conditions in porous media. The surfactant concentration is 0.1 wt%.

than CMC. At greater surfactant concentrations and with increasing liquid and gas velocities, the pressure gradient contours change dramatically and even transform into V-shaped contours.

Moreover, it is also found that with increasing surfactant concentration, the density of pressure gradient contours near the axis of the gas Darcy velocity increases. It shows that the sensitivity of pressure gradient to liquid velocity increases with the increase of surfactant concentration in the low-liquid velocity range. Fig. 6 illustrates the main concept considered to analyze the evolution of the pressure gradient contours in the following sections. The effects of gas and liquid velocity were studied according to the dotted line named Fixed U_g varying U_w, and the effects of foam quality were studied according to the dotted line named Fixed U_t varying f_g in Fig. 6.

3.2. Effects of gas and liquid velocity

Gas and liquid velocities affect the foam quality and stability of lamellae. The pressure gradient as a function of the liquid velocity at 3 fixed gas velocities of 1, 8, and 16 m/day at different surfactant concentrations was investigated.

It is found that when the surfactant concentration reaches the CMC, the pressure gradient increases first and then decreases with the increase of liquid velocity for a constant gas velocity. The foam flow resistance is very sensitive to the number and shape of lamellae. At a liquid velocity of 0 m/day, the flow in porous media is single-phase gas flow, and the pressure gradient is very low. At a fixed gas velocity and a certain surfactant concentration, with increasing liquid velocity from 0 m/day, an increasing amount of liquid is available to generate lamellae. Accordingly, the pressure gradient increases quickly and then peaks. At the peak of the pressure gradient, the lamellae are very thin, as shown in Fig. 7a, and the capillary pressure reaches the limiting capillary pressure. With a further increase in the liquid velocity, the capillary pressure decreases, and the lamellae become thicker and evolve into lenses, as shown in Fig. 7b. The flow resistance in Fig. 7a is greater than that in Fig. 7b. Therefore, the pressure gradient decreases from the peak point.

As foam flows through porous media, the wetting liquid phase occupies the smallest pore spaces. Some gas (foam) flows through the large pore spaces, while some gas is trapped in the intermediate-sized pore spaces (Radke and Gillis, 1990). According to this phenomenon, Rossen and Wang reported the steady-state phase distribution at a foam quality of 85% as a broad log-normal tube-radius distribution. As the lamellae change into lenses, the flow resistance declines, and a portion of the trapped gas transitions into flowing gas. Moreover, if the liquid velocity increases further, the capillary pressure continues to decrease, and water imbibes into intermediate-sized pores occupied by trapped gas (Rossen and Wang, 1997). Accordingly, the liquid relative permeability increases, and gas flows through a greater fraction or almost the same fraction of larger pores. Therefore, there occurs a slight decline or no change in the pressure gradient.

At a small gas velocity such as 1 m/day, the flow regime struggles to reach the limiting capillary pressure because the foam is very wet. Hence, it is rare to observe a decline in the pressure gradient with increasing liquid velocity. Therefore, the pressure gradient contours near the coordinate axis remain L-shaped but change into V-shaped in the other regions when the surfactant concentration reaches the CMC, which is consistent with the results of the previous section.

Meanwhile, it is found that when the surfactant concentration reaches the CMC, the peak point of the pressure gradient occurs at smaller liquid velocity as the surfactant concentration increases. At the gas velocity $v_g = 16$ m/day, the peak point of the pressure gradient occurs at the liquid velocity of 8 m/day when the surfactant concentration is 0.1 wt%, but at the liquid velocity of 2 m/day when the surfactant concentration is 0.5 or 0.7 wt%. Surfactant concentration has a significant influence on the transient foam behavior or foam generation (Kahrobaei and Farajzadeh, 2019). The rate of foam generation increases with the increase of the surfactant concentration. So stable foam can be produced at a small liquid velocity, and the peak pressure gradient can be reached. This also explains why the density of pressure gradient contours near the axis of the gas Darcy velocity increased as the surfactant concentration increased in the previous section.

It is also found that when the surfactant concentration is less than the CMC, the gas-liquid system does not generate stable lamellae, so the pressure gradient increases gradually as liquid velocity increases for a constant gas velocity. At small surfactant concentrations, the limiting capillary pressure declines. The gas-liquid system does not generate stable thin lamellae as shown in Fig. 7a. Therefore, the bubbles are separated by lenses, as shown in Fig. 7b. Moreover, there are few bubbles trapped in intermediate-sized pores resulting in a

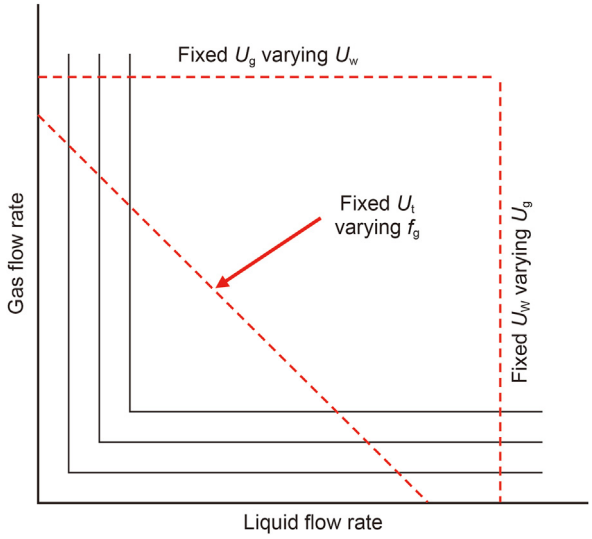

Fig. 6. Illustration of the main concept to analyze the evolution of the pressure gradient contours (Alvarez et al., 2001).

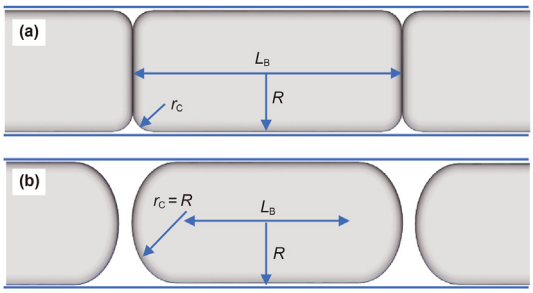

Fig. 7. Bubble configuration when bubbles are separated by lamellae at high-foam quality (**a**) and lenses at low-foam quality (**b**).

small to moderate flow resistance, especially at a greater total flow rate. Fig. 8 shows the pressure gradient as a function of the liquid velocity at 3 fixed gas velocities at a surfactant concentration of 0.01 wt%. At smaller liquid velocities, bubbles are trapped in intermediate-sized pores. Therefore, the pressure gradient slightly declines or remains constant as more intermediate-sized pores become occupied by liquid with increasing liquid velocity. When few bubbles are trapped in the pores and liquid does not occupy proportionally more pores with increasing liquid velocity, the pressure gradient increases. At large liquid velocities and smaller foam qualities, few bubbles are trapped in the pores and flow occurs with increasing liquid content. Therefore, the pressure gradient increases with increasing liquid velocity such as at $v_g = 16$ m/day in Fig. 8.

3.3. Effects of foam quality

Foam quality is a key parameter characterizing foam flow in porous media. Given a particular porous medium, the effects of the foam quality on the resultant flow characteristics change with other factors. Fig. 9 shows the pressure gradient as a function of the foam quality at the same total velocity of 10 m/day. Generally, the pressure gradient first increases with increasing foam quality, reaches a maximum value, and then decreases with increasing foam quality.

At a low-foam quality, bubbles are trapped in intermediate-sized pores, and the remaining bubbles flow through the largest pores (Kovscek et al., 1997). Liquid slugs (lenses or lamellae) occur between adjacent bubbles, as shown in Fig. 7b. The number of lamellae or lenses per unit capillary length is the most important variable affecting the foam flow resistance. More lamellae or lenses

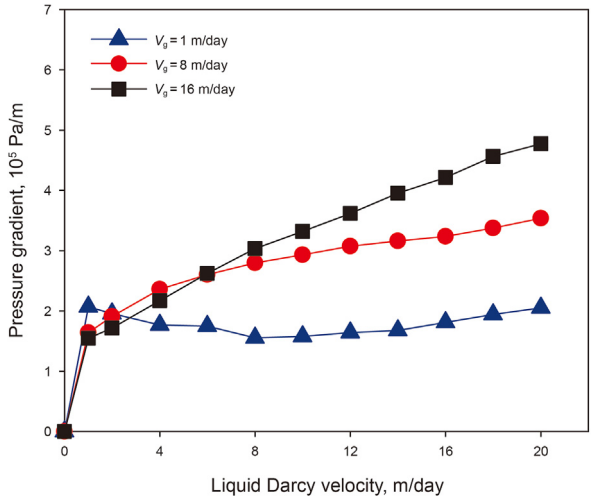

Fig. 8. Pressure gradient as a function of the liquid Darcy velocity at different gas Darcy velocities under steady-state conditions in porous media. The surfactant concentration is 0.01 wt%.

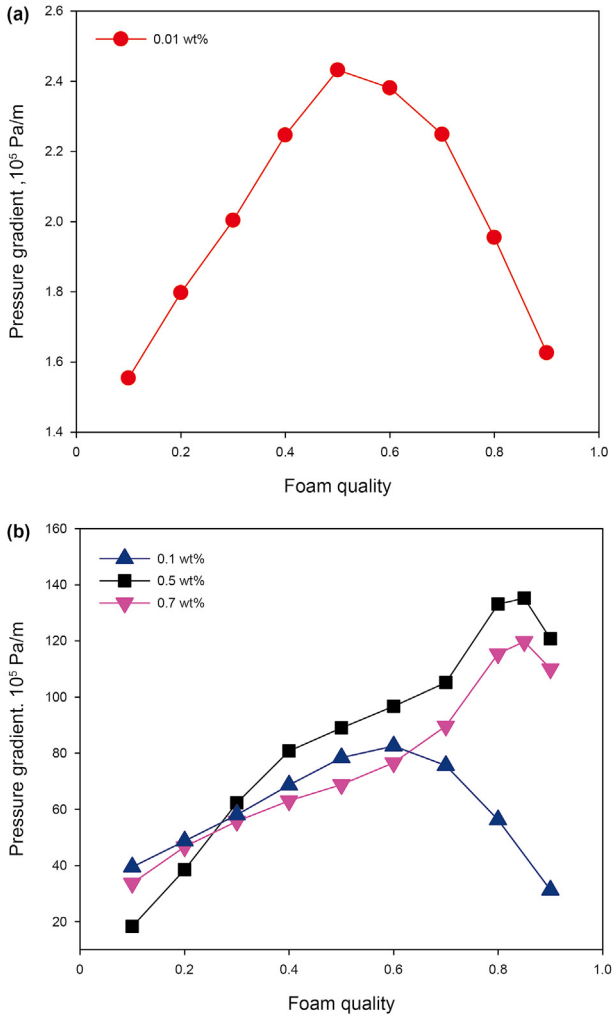

Fig. 9. Pressure gradient as a function of the foam quality under steady-state conditions in porous media at different surfactant concentrations. The liquid and gas total Darcy velocities are all 10 m/day. The surfactant concentrations are: (**a**) 0.01 wt%; (**b**) 0.1, 0.5, and 0.7 wt%.

per unit length result in a greater flow resistance. With increasing foam quality, the flow resistance increases as a consequence of an increase in the number of lamellae increase, as shown in Fig. 9. With increasing foam quality, the capillary pressure increases and reaches the limiting capillary pressure thereby leading to foam coalescence and a decline in the number of lamellae per unit length. If the foam quality increases, the regime transforms into the high-quality region. Liquid reduction results in a decrease in lamellae and bubble enlargement, and the number of lamellae per unit length declines. Therefore, the flow resistance decreases with increasing foam quality after regime transition.

There exists a certain foam quality corresponding to the maximum flow resistance in a particular flow system, called transition foam quality. The transition points between foam regimes vary with the different surfactant concentrations. Usually, the transition point occurs at a greater foam quality as surfactant concentration increases. As shown in Fig. 9, the transition foam quality is approximately 0.5 at a surfactant concentration of 0.01 wt %. This value changes to approximately 0.6 at 0.1 wt% and reaches 0.84 at surfactant concentrations of 0.5 and 0.7 wt%. This indicates that a greater surfactant concentration better stabilizes lamellae at a high-foam quality, and the limiting capillary pressure increases with increasing surfactant concentration.

According to the dotted line named Fixed U_t varying f_g in Fig. 6, the foam quality increases from the lower right area of the dotted line to the upper left area at the same total velocity of 10 m/day. As surfactant concentration increases, the transition foam quality increases, and the transition point corresponding to the maximum flow resistance is closer to the axis of the gas Darcy velocity. Therefore, the density of pressure gradient contour lines near the axis of the gas Darcy velocity increases with increasing surfactant concentration. The evolution of the transition foam quality with surfactant concentration also results in V-shaped curves in the high gas and liquid velocities region when the surfactant concentration reaches CMC.

4. Conclusions

In this study, serval experiments of foam flow in porous media by injecting pre-generated N_2 foam into a sand pack under the condition of considering a wide range of gas/liquid velocities and surfactant concentrations were conducted. For the experimental results and under our experimental conditions, the following conclusions are made:

(1) The pressure gradient during foam flow through porous media under steady-state conditions is a function of the liquid and gas Darcy velocities. Over a wide range of velocities, the pressure gradient contours are L-shaped near the coordinate axes when gas velocity versus liquid velocity is plotted. Contours evolve from L-shaped into V-shaped in other regions. This evolution is an indication of complex foam rheology that is a function of the texture of foam bubbles.

(2) The surfactant concentration has a great impact on the stability of foam in porous media. The maximum pressure gradient under steady state conditions increases with increasing surfactant concentration, especially as the concentration reaches the CMC.

(3) Foam flow resistance and the shape and magnitude of the pressure gradient contours are very sensitive to the surfactant concentration in both the high- and low-foam quality regime, especially when the surfactant concentration is less than the CMC. When the surfactant concentration is less than the CMC, the gas-liquid system does not generate stable lamellae, so the pressure gradient increases gradually as liquid velocity increases for a constant gas velocity. However, when the surfactant concentration reaches the CMC, the pressure gradient increases first and then decreases with the increase of liquid velocity, which also reflects the transition from high-to low-quality regime of foam.

(4) The foam quality is an important variable to the flow resistance obtained. There exists a certain foam quality corresponding to the maximum flow resistance in a particular flow system, called transition foam quality. Usually, the transition point occurs at a greater foam quality as surfactant concentration increases.

(5) Due to the limitation of the size of the sand pack tested, we only evaluated the flow characteristics of foam in porous media by measuring its pressure drop, which had some limitations. It is still not clear how pressure gradients are established for steady flow of foam in porous media, especially over a wide range of gas/liquid velocities and surfactant concentrations.

Declaration of competing interest

The authors declare that they have no known competing financial interests or personal relationships that could have appeared to influence the work reported in this paper.

Acknowledgments

This project was financially supported by National Natural Science Foundation of China (No. U20B6003). We are grateful to the researchers at the Foam Fluid Enhanced Oil & Gas Production Engineering Research Center of China University of Petroleum (East China) and Department of Energy Resources Engineering of Stanford University for their kind help in this study.

Appendix

The pressure gradient respectively reaches 180 $\times$ 10^5 and 190 $\times$ 10^5 Pa/m within the measurement range at surfactant concentrations of 0.5 and 0.7 wt% (Fig. A.1).

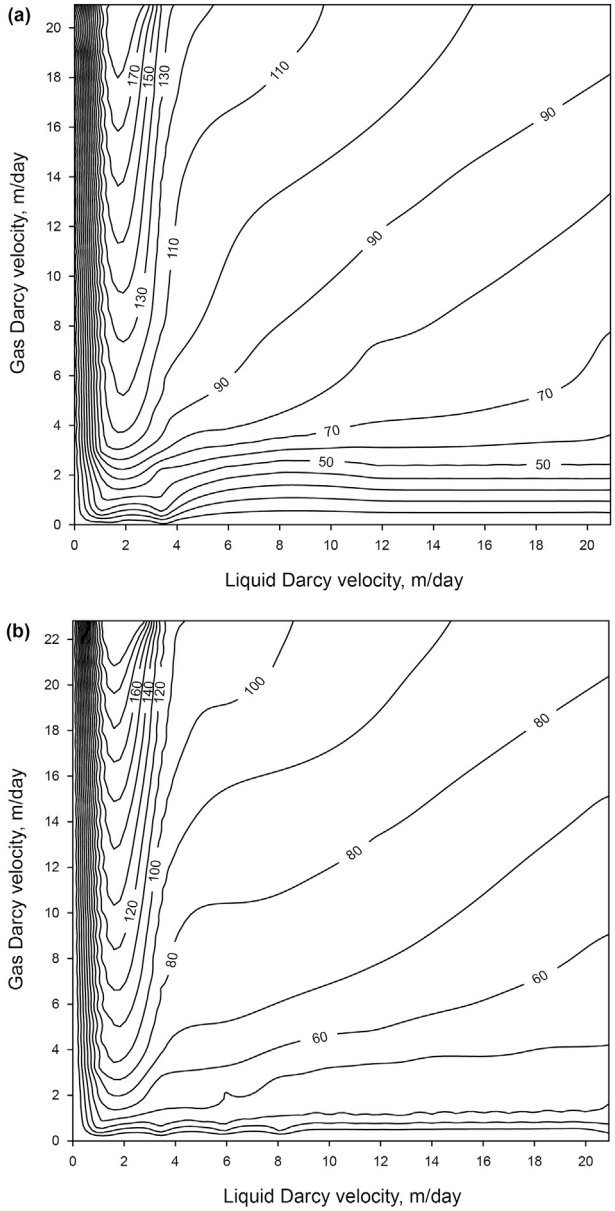

Fig. A.1. Pressure gradient contours (10^5 Pa/m) as a function of the liquid Darcy velocity (m/day) and gas Darcy velocity (m/day) under steady-state conditions in porous media at different surfactant concentration. The surfactant concentrations are: (**a**) 0.5 wt%; (**b**) 0.7 wt%.

When the surfactant concentration reaches the CMC, the pressure gradient increases first and then decreases with the increase of liquid velocity for a constant gas velocity (Fig. A.2).

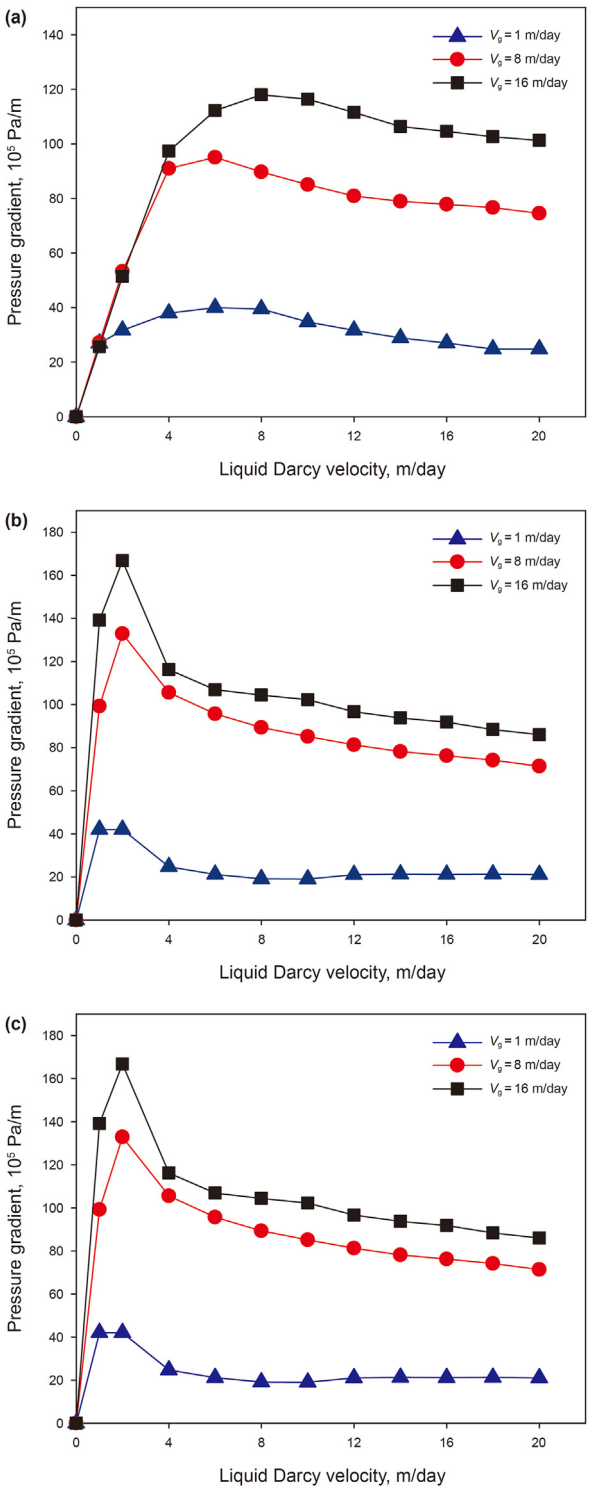

Fig. A.2. Pressure gradient as a function of the liquid Darcy velocity at different gas Darcy velocities under steady-state conditions in porous media at different surfactant concentrations. The surfactant concentrations are: (**a**) 0.1 wt%; (**b**) 0.5 wt%; (**c**) 0.7 wt%.

References

Adebayo, A.R., Kanj, M.Y., 2018. Exploring a mechanistic approach for characterizing transient and steady state foam flow in porous media. J. Nat. Gas Sci. Eng. 60, 214–227. https://doi.org/10.1016/j.jngse.2018.10.016.

Almajid, M.M., Kovscek, A.R., 2022. Experimental investigation of transient foam flow in a long heterogeneous consolidated sandstone. In: SPE Improved Oil Recovery Conference. Society of Petroleum Engineers. https://doi.org/10.2118/209401-MS.

Alvarez, J.M., Rivas, H.J., Rossen, W.R., 2001. Unified model for steady-state foam behavior at high and low foam qualities. SPE J. 6 (3), 325–333. https://doi.org/10.2118/74141-PA.

Buchgraber, M., Castanier, L.M., Kovscek, A.R., 2012. Microvisual investigation of foam flow in ideal fractures: role of fracture aperture and surface roughness. In: SPE Annual Technical Conference and Exhibition. Society of Petroleum Engineers. https://doi.org/10.2118/159430-MS.

Chen, L.K., Huang, M.M., Li, Z.M., Liu, D.J., Li, B.F., 2019. Experimental study on the characteristics of foam flow in fractures. J. Pet. Sci. Eng. 185, 106663. https://doi.org/10.1016/j.petrol.2019.106663.

Cheng, L., Reme, A.B., Shan, D., Coombe, D.A., 2000. Simulating foam processes at high and low foam qualities. In: SPE/DOE Improved Oil Recovery Symposium. Society of Petroleum Engineers. https://doi.org/10.2118/59287-MS.

Ding, M.C., Li, Q., Yuan, Y.J., Wang, Y.F., Zhao, N., Han, Y.G., 2021. Permeability and heterogeneity adaptability of surfactant-alternating-gas foam for recovering oil from low-permeability reservoirs. Petrol. Sci. 19 (3), 1185–1197. https://doi.org/10.1016/j.petsci.2021.12.018.

Farajzadeh, R., Lotfollahi, M., Eftekhari, A.A., Rossen, W.R., Hirasaki, J.H., 2015. Effect of permeability on implicit-texture foam model parameters and the limiting capillary pressure. Energy Fuel. 29 (5), 3011–3018. https://doi.org/10.1021/acs.energyfuels.5b00248.

Fernø, M.A., Eide, Ø., Steinsbø, M., Langlo, S.A.W., Christophersen, A., Skibenes, A., Ydstebø, T., Graue, A., 2015. Mobility control during CO_2 EOR in fractured carbonates using foam: laboratory evaluation and numerical simulations. J. Pet. Sci. Eng. 135, 442–451. https://doi.org/10.1016/j.petrol.2015.10.005.

Fernø, M.A., Gauteplass, J., Pancharoen, M., Haugen, A., Graue, A., Kovscek, A.R., Hirasaki, G., 2016. Experimental study of foam generation, sweep efficiency, and flow in a fracture network. SPE J. 21 (4), 1140–1150. https://doi.org/10.2118/170840-PA.

Gauteplass, J., Chaudhary, K., Kovscek, A.R., Fernø, M.A., 2015. Pore-level foam generation and flow for mobility control in fractured systems. Colloid. Surf. Physicochem. Eng. Asp. https://doi.org/10.1016/j.colsurfa.2014.12.043.

Hematpur, H., Mahmood, S.M., Nasr, N.H., Elraies, K.A., 2018. Foam flow in porous media: concepts, models and challenges. J. Nat. Gas Sci. Eng. 53, 163–180. https://doi.org/10.1016/j.jngse.2018.02.017.

Johnson, P., Starov, V., Trybala, A., 2022. Foam flow through porous media. Curr. Opin. Colloid Interface Sci. 58, 101555. https://doi.org/10.1016/j.cocis.2021.101555.

Kahrobaei, S., Farajzadeh, R., 2019. Insights into effects of surfactant concentration on foam behavior in porous media. In: IOR 2019–20th European Symposium on Improved Oil Recovery. European Association of Geoscientists & Engineers. https://doi.org/10.3997/2214-4609.201900252.

Kahrobaei, S., Vincent-Bonnieu, S., Farajzadeh, R., 2017. Experimental study of hysteresis behavior of foam generation in porous media. Sci. Rep. 7, 8986. https://doi.org/10.1038/s41598-017-09589-0.

Kam, S.I., Frenier, W.W., Davies, S.N., Rossen, W.R., 2007. Experimental study of high-temperature foam for acid diversion. J. Pet. Sci. Eng. 58 (1–2), 138–160. https://doi.org/10.1016/j.petrol.2006.12.005.

Khatib, Z.I., Hirasaki, G.J., Falls, A.H., 1988. Effects of capillary pressure on coalescence and phase mobilities in foams flowing through porous media. SPE Reservoir Eng. 3, 919–926. https://doi.org/10.2118/15442-PA.

Kovscek, A.R., Patzek, T.W., Radke, C.J., 1997. Mechanistic foam flow simulation in heterogeneous and multidimensional porous media. SPE J. 2 (4), 511–526. https://doi.org/10.2118/39102-PA.

Li, B.F., Li, Z.M., Lv, Q.C., Zhang, H.S., Zhang, Y., 2017. Physical simulation on flowing characteristics of foam in fracture. J. Cent. South Univ. 48 (9), 2465–2473. https://doi.org/10.11817/j.issn.1672-7207.2017.09.027.

Li, B.F., Li, H.F., Cao, A.Q., Wang, F., 2019. Effect of surfactant concentration on foam texture and flow characteristics in porous media. Colloid. Surf. Physicochem. Eng. Asp 560 (5), 189–197. https://doi.org/10.1016/j.colsurfa.2018.10.027.

Lozano, L.F., Zavala, R.Q., Chapiro, G., 2021. Mathematical properties of the foam flow in porous media. Comput. Geosci. 25, 515–527. https://doi.org/10.1007/s10596-020-10020-3.

Lv, Q.C., Li, Z.M., Li, B.F., Husein, M., Shi, D.S., Zhang, C., 2017. Wall slipping behavior of foam with nanoparticle-armored bubbles and its flow resistance factor in cracks. Sci. Rep. 7 (1), 1–14. https://doi.org/10.1038/s41598-017-05441-7.

Omirbekov, S., Davarzani, H., Ahmadi-Senichault, A., 2020. Experimental study of non-Newtonian behavior of foam flow in highly permeable porous media. Ind. Eng. Chem. Res. 59 (27), 12568–12579. https://doi.org/10.1021/acs.iecr.0c00879.

Osterloh, W.T., Jante, M.J., 1992. Effects of gas and liquid velocity on steady-state foam flow at high temperature. In: SPE/DOE Enhanced Oil Recovery

Symposium. Society of Petroleum Engineers. https://doi.org/10.2118/24179-MS.
Radke, C.J., Gillis, J.V., 1990. A dual gas tracer technique for determining trapped gas saturation during steady foam flow in porous media. In: SPE Annual Technical Conference and Exhibition. Society of Petroleum Engineers. https://doi.org/10.2118/20519-MS.
Roncoroni, M.A., Romero, P., Montes, J., Bascialla, G., Rodríguez, R., Pons-Esparver, R.R., Mazadiego, L.F., García-Mayoral, M.F., 2021. Enhancement of a foaming formulation with a zwitterionic surfactant for gas mobility control in harsh reservoir conditions. Petrol. Sci. 18 (5), 1409–1426. https://doi.org/10.1016/j.petsci.2021.08.004.
Rossen, W.R., Wang, M.W., 1997. Modeling foams for acid diversion. In: SPE European Formation Damage Conference. Society of Petroleum Engineers. https://doi.org/10.2118/38200-MS.
Rudyk, S., Al-Khamisi, S., Al-Wahaibi, Y., 2020. Governing factors of foam flow in porous media of Berea sandstone at 1–8% NaCl. J. Nat. Gas Sci. Eng. 83, 103528. https://doi.org/10.1016/j.jngse.2020.103528.
Sarhan, A.R., Naser, J., Brooks, G., 2016. CFD simulation on influence of suspended solid particles on bubbles' coalescence rate in flotation cell. Int. J. Miner. Process. 146, 54–64. https://doi.org/10.1016/j.minpro.2015.11.014.
Sarhan, A.R., Naser, J., Brooks, G., 2017a. CFD analysis of solid particles properties effect in three-phase flotation column. Separ. Purif. Technol. 185, 1–9. https://doi.org/10.1016/j.seppur.2017.04.042.
Sarhan, A.R., Naser, J., Brooks, G., 2017b. Numerical simulation of froth formation in aerated slurry coupled with population balance modelling. Can. Metall. Q. 56 (1), 45–57. https://doi.org/10.1080/00084433.2016.1268771.
Sarhan, A.R., Naser, J., Brooks, G., 2017c. CFD Modeling of three-phase flotation column incorporating a population balance model. Procedia Eng. 184, 313–317. https://doi.org/10.1016/j.proeng.2017.04.100.
Sarhan, A.R., Naser, J., Brooks, G., 2018a. Effects of particle size and concentration on bubble coalescence and froth formation in a slurry bubble column. Particuology 36, 82–95. https://doi.org/10.1016/j.partic.2017.04.011.
Sarhan, A.R., Naser, J., Brooks, G., 2018b. CFD model simulation of bubble surface area flux in flotation column reactor in presence of minerals. Int. J. Min. Sci. Technol. 28 (6), 999–1007. https://doi.org/10.1016/j.ijmst.2018.05.004.
Sarhan, A.R., Naser, J., Brooks, G., 2018c. Bubbly flow withparticle attachment and detachment – a multi-phase CFD study. Separ. Sci. Technol. 53 (1), 181–197. https://doi.org/10.1080/01496395.2017.1375525.
Sarhan, A.R., Naser, J., Brooks, G., 2018d. CFD modeling of bubble column: influence of physico-chemical properties of the gas/liquid phases properties on bubble formation. Separ. Purif. Technol. 201, 130–138. https://doi.org/10.1016/j.seppur.2018.02.037.
Simjoo, M., Zitha, P.L.J., 2020. Modeling and experimental validation of rheological transition during foam flow in porous media. Transport Porous Media 131, 315–332. https://doi.org/10.1007/s11242-019-01251-9.
Singh, R., Mohanty, K.K., 2017. Foam flow in a layered, heterogeneous porous medium: a visualization study. Fuel 197, 58–69. https://doi.org/10.1016/j.fuel.2017.02.019.
Skauge, A., Solbakken, J., Ormehaug, P.A., Aarra, M.G., 2020. Foam generation, propagation and stability in porous medium. Transport Porous Media 131, 5–21. https://doi.org/10.1007/s11242-019-01250-w.
Sun, Y.P., Xin, Y., Lyu, F.T., Dai, C.L., 2021. Experimental study on the mechanism of adsorption-improved imbibition in oil-wet tight sandstone by a nonionic surfactant for enhanced oil recovery. Petrol. Sci. 18 (4), 1115–1126. https://doi.org/10.1016/j.petsci.2021.07.005.
Tang, J.Y., Vincent-Bonnieu, S., Rossen, W.R., 2019. Experimental investigation of the effect of oil on steady-state foam flow in porous media. SPE J. 24 (1), 140–157. https://doi.org/10.2118/194015-PA.
Wang, C., Li, H.A., 2016. Stability and mobility of foam generated by gas-solvent/surfactant mixtures under reservoir conditions. J. Nat. Gas Sci. Eng. 34, 366–375. https://doi.org/10.1016/j.jngse.2016.06.064.
Wang, F., Du, D.X., Chen, H.L., Zhang, C., 2019. Simulation of evolution mechanism of dynamic interface of aqueous foam in narrow space base on level set method. Colloid. Surf. Physicochem. Eng. Asp. 574, 1–11. https://doi.org/10.1016/j.colsurfa.2019.04.004.
Wang, Z.J., Li, S.Y., Li, Z.M., 2022. A novel strategy to reduce carbon emissions of heavy oil thermal recovery: condensation heat transfer performance of flue gas-assisted steam flooding. Appl. Therm. Eng. 205, 118076. https://doi.org/10.1016/j.applthermaleng.2022.118076.
Yu, G.Q., Vincent-Bonnieu, S., Rossen, W.R., 2020. Foam propagation at low superficial velocity: implications for long-distance foam propagation. SPE J. 25 (6), 3457–3471. https://doi.org/10.2118/201251-PA.